AAPG International Conference
Barcelona, Spain
September 21-24, 2003

Jose Agnelo Soares[1], Margareth da Silva Brasil Guimaraes[1] (1) Rio de Janeiro Federal University, Rio de Janeiro, Brazil

Using Thomsen's Model to Analyze Composition and Internal Structure of Shales

Abstract

In terms of seismic wave propagation shale may be treated as a VTI medium. This is a homogeneous transversely isotopic medium whose axis of symmetry is vertical. In other words, it is assumed that shale horizontal bedding is a result of hard and soft platelets interlamination. Hard platelets may be composed of hard minerals like quartz or some clay minerals, whereas soft ones are filled of organic matter and its fluids. For a VTI medium there are three mutually independent phase velocities (V_P, V_{SH} and V_{SV}) and five stiffness components (c_{11}, c_{12}, c_{33}, c_{44} and c_{13}). Thomsen suggested replacing these stiffness components with two vertical velocities (V_{P0} and V_{S0}) and three dimensionless anisotropy parameters (γ, ε and δ). The γ parameter depends on Poisson´s ratio of the solid and on the ratio of the soft platelets porosity over their aspect ratio, but e and d parameters are, additionally, functions of fluid/solid bulk modulus ratio and soft platelets porosity. Thus, knowing the anisotropy Thomsen´s parameters through wave velocities measurements in shale samples and adopting a value for soft platelets aspect ratio, fluid/solid bulk modulus ratio and soft platelets porosity can be determined. Finally, these variables may be analyzed in terms of mineral/organic composition, fluid saturation and spatial internal structure of shales.

Introduction

Homogeneous materials that exhibit hexagonal elastic anisotropy can be completely represented by five independent elastic constants: c_{11}, c_{12}, c_{33}, c_{44} and c_{13}. Shales present horizontal bedding what allow their classification as VTI media. VTI media, a subclass of hexagonal anisotropy, are characterized by isotropy around a vertical axis, as in the shale case. Using shale plugs cut parallel, perpendicular and 45 degrees from bedding plane, the five elastic constants are obtained (Johnston & Christensen, 1995). Assuming plane containing axis 1 and 2 as the plane parallel to shale bedding (with axis 3 perpendicular to this plane) and doing laboratory measurements of P wave velocity in direction parallel V_{Ppar}, perpendicular V_{Pper} and 45 degrees from shale bedding V_{P45}, plus S wave axial velocity measurements in plugs cut perpendicular V_{S0} and parallel to shale bedding V_{S90}:

$$
\begin{aligned}
c_{11} &= \rho\, V_{P\,par}^2 \\
c_{33} &= \rho\, V_{P\,per}^2 \\
c_{44} &= \rho\, V_{S0}^2 \\
c_{12} &= c_{11} - 2\rho\, V_{S90}^2 \\
c_{13} &= -c_{44} + \left[\begin{matrix} 4\rho^2 V_{P45}^4 - 2\rho V_{P45}^2 (c_{11} + c_{33} + 2c_{44}) + \\ + (c_{11} + c_{44})(c_{33} + c_{44}) \end{matrix} \right]^{1/2}
\end{aligned}
\qquad (1)
$$

where ρ is the rock sample density.

According Thomsen (1986, 1995) a VTI medium presents the following phase velocities as function of angle Q (defined as the angle between symmetry axis and the direction of wave propagation):

$$V_P^2(\Theta) = V_{P0}^2\left(1 + 2\delta\sin^2\Theta\cos^2\Theta + 2\varepsilon\sin^4\Theta\right)$$
$$V_{SV}^2(\Theta) = V_{S0}^2\left[1 + 2\frac{V_{P0}^2}{V_{S0}^2}(\varepsilon - \delta)\sin^2\Theta\cos^2\Theta\right] \qquad (2)$$
$$V_{SH}^2(\Theta) = V_{S0}^2\left(1 + 2\gamma\sin^2\Theta\right)$$

where V_{P0} e V_{S0} are P and S wave velocities when $\Theta = 0$, VSV is the S wave velocity polarized in vertical direction, V_{SH} is the S wave velocity horizontally polarized, and

$$\varepsilon \equiv \frac{c_{11} - c_{33}}{2c_{33}}$$
$$\gamma \equiv \frac{\left(\frac{c_{11} - c_{12}}{2}\right) - c_{44}}{2c_{44}} \qquad (3)$$
$$\delta \equiv \frac{(c_{13} + c_{44})^2 - (c_{33} - c_{44})^2}{2c_{33}(c_{33} - c_{44})}$$

are parameters which define the shape of P and S wave velocity surfaces.

Therefore, knowing the five elastic constants, which may be calculated from the elastic velocities V_{Ppar}, V_{Pper}, V_{P45}, V_{S0} and V_{SH}, one can also obtain the Thomsen´s anisotropy parameters ε, γ and δ.

Otherwise, Thomsen (1995) also presented these anisotropy parameters as function of petrophysical variables which allow an interpretation about composition and internal structure of the rock in analysis. In this work anisotropy parameters calculated from petrophysical variables are marked with asterisk to distinguish from those calculated from elastic constants (equations 3). Thomsen considered the case of anisotropy caused by a set of fractures aligned in a given direction, with fracture pore space (secondary porosity) fluid filled and whose fluid interacts with rock primary porosity. Assuming that fractures have the shape of circular ellipsoids and low primary porosity values, the petrophysical anisotropy parameters are given by

$$\varepsilon^* = \frac{8}{3}\left(1 - \frac{K_f}{K_s}\right)D_{cp}\,\eta_c$$
$$\gamma^* = \frac{8}{3}\left(\frac{1 - \nu_s}{2 - \nu_s}\right)\eta_c \qquad (4)$$
$$\delta^* = 2(1 - \nu_s)\varepsilon - 2\left(\frac{1 - 2\nu_s}{1 - \nu_s}\right)\gamma$$

where ν_S is the Poisson´s ratio of solid frame and K_f and K_S are fluid and solid bulk modulus, respectively. D_{cp} is a factor of fluid influence which, for relatively high frequency as used in laboratory ultrasonic measurements, is given by

$$D_{cp} = \left[1 - \frac{K_f}{K_s} + \frac{K_f}{K_s\,\phi_c}\{A_c(\nu_s)\eta_c\}\right]^{-1}$$

where ϕ_c is the secondary porosity (fracture porosity) and

$$A_c(\nu_s)\eta_c = \frac{16}{9}\left(\frac{1-\nu_s^2}{1-2\nu_s}\right)\eta_c$$

η_c is the medium fracture density which is given by

$$\eta_c = \frac{3}{4\pi}\frac{\phi_c}{(c/a)}$$

and (c/a) is the fracture aspect ratio (thickness/diameter).

Proposed Method

This work presents a method for using of the Thomsen´s model to evaluate rock composition and internal structure of shales through substitution of the medium containing aligned fractures fluid filled by another equivalent medium. This equivalent medium is the shale, formed by a solid frame with interlaminations of aligned ellipsoidal inclusions. Hard mineral like quartz and some clay minerals form the mineral frame whereas ellipsoidal inclusions are formed of organic matter and fluids.

Substituting η_c in γ^* equation (eq. 4) and after some necessary handling, the following expression is achieved for the new variable $R_c = \phi_c/(c/a)$:
Considering that γ value, derived from measured elastic constants, is equal to γ^*, for any value of ν_s the

$$R_c = \frac{\pi\gamma^*(2-\nu_s)}{2(1-\nu_s)} \qquad (5)$$

correspondent R_c value may be calculated.

On the other hand, substituting D_{cp} and η_c in ε expression (eq. 4) and after some algebraic manipulation, may be written

$$\varepsilon^* = \frac{2R_c(1-K_r)}{\pi(1-K_r)+K_r\left[\frac{4(1-\nu_s^2)}{3(c/a)(1-2\nu_s)}-\pi\right]}$$

or

$$K_r = \frac{2R_c-\pi\varepsilon^*}{\varepsilon^*\left[\frac{4(1-\nu_s^2)}{3(c/a)(1-2\nu_s)}-\pi\right]+2R_c} \qquad (6)$$

where $K_r = K_f / K_s$.

Here we proposes to use equations (5) and (6) in iterative way. In other words, doing ν_s value varies from 0.00 up to 0.50 in steps of 0.01, for each value of ν_s corresponding values for R_c and K_r are calculated. Initially, a value for the aspect ratio of organic inclusions must be assumed. Thereafter, using equations (4), corresponding ε^*, γ^* and δ^* parameters are calculated, comparing the δ^* value with the value of corresponding original parameter δ. When δ^* and δ values converge to a unique number, values for variables ν_s, R_c and K_r are established which honor the pattern of seismic anisotropy observed in the rock sample.

Example of method application

Johnston and Christensen (1995) measured, in laboratory, all the five seismic velocities which are sufficient to

Table 1 - Sample composition (modified from Johnston & Christensen, 1995).

Sample	Silica (%)	Clays (%)	Carbonate (%)	Organic Matter (%)
TH-26	48.80	31.58	0.10	19.52
TH-51	51.58	31.56	0.05	16.81
NEW-2	65.59	20.85	0.06	13.50
NEW-3	63.03	21.81	1.16	14.00
NEW-5	62.15	20.12	2.97	14.76
NEW-7	60.55	20.83	3.92	14.70
ANT-1	58.25	21.88	0.37	19.50

Table 2 - Calculated petrophysical parameters.

Sample	Pressure (MPa)	ν_s	K_f / K_s	ϕ_c (%)
TH-26	10	0.36	0.12703	31.8
	50	0.42	0.10322	30.6
	100	0.42	0.10972	29.5
TH-51	10	0.33	0.13287	27.5
	50	0.33	0.14607	27.3
	100	0.34	0.15347	26.9
NEW-2	10	0.10	0.13617	11.2
	50	0.36	0.10177	12.3
	100	0.39	0.09017	11.6
NEW-3	10	0.21	0.09653	12.1
	50	0.36	0.08963	12.9
	100	0.37	0.09311	12.2
NEW-5	10	0.37	0.05125	11.4
	50	0.38	0.06875	11.1
	100	0.40	0.06675	10.6
NEW-7	10	0.39	0.05925	11.8
	50	0.35	0.08825	10.6
	100	0.35	0.09475	10.1
ANT-1	10	0.41	0.07175	16.9
	50	0.39	0.09825	15.5
	100	0.38	0.11625	14.9

calculate the five elastic constants of shale samples collected from seven outcrops. The seismic velocities of each sample were measured under three different levels of hydrostatic pressure. Additionally, sample composition was analyzed through x ray diffraction and electronic microscopy.

The results of Johnston and Christensen (1995) are used in this work to exemplify how the method presented here can be applied to evaluate composition and internal structure of shales.

Table 1 gives an author's interpretation for approximated mineralogical composition of Johnston & Christensen's shale samples. For this interpretation it was assumed clay content as the sum of Al_2O_3, Fe_2O_3 and MgO contents, carbonate content as equal to CaO one and, finally, organic matter content as being equal to all remainder, which includes matter lost in ignition, fluids and trace elements.

Assuming an aspect ratio value of 1/10 for the organic matter inclusions, or in other words, considering inclusions with approximated shape of flattened ellipsoids whose diameter corresponds to ten times their thickness, and applying the proposed method for evaluation of composition and internal structure of shales, results presented in Table 2 were obtained.

Using the petrophysical parameters showed in Table 2, phase velocities traveling in any arbitrary vertical plane of each shale sample were calculated. These velocities change with angle Θ measured between the isotropy axis (vertical) and the direction of wave propagation. Figure 1 depicts the wave velocities that propagate in a vertical plane of sample TH-26 as function of angle Θ. In Figure 2 these velocities are exhibited as a map in polar coordinates. In these figures colors blue, green and red indicate hydrostatic pressure of 10 MPa, 50 MPa and 100 MPa, respectively. The other samples showed similar behavior.

As can be seen in Figure 2, a VTI anisotropy medium presents maximum and minimum values for P and Sh wave velocities at Θ equal to 90º and 0º, respectively. In the case of S_V wave these extreme values occur when Θ is equal to 45º and 0º. Defining wave velocity anisotropy as $(V_{max} - V_{min})/V_{max}$ in percent, and using the petrophysical parameters listed in Table 2, the anisotropy values for P, Sh and Sv waves presented in Table 3 were achieved.

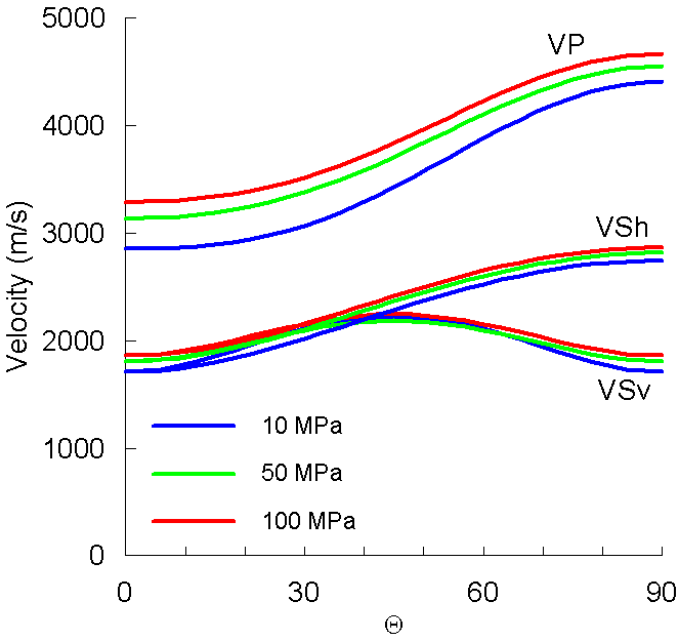

Figure 1 - Velocities of waves propagating in a vertical plane of TH-26 shale sample.

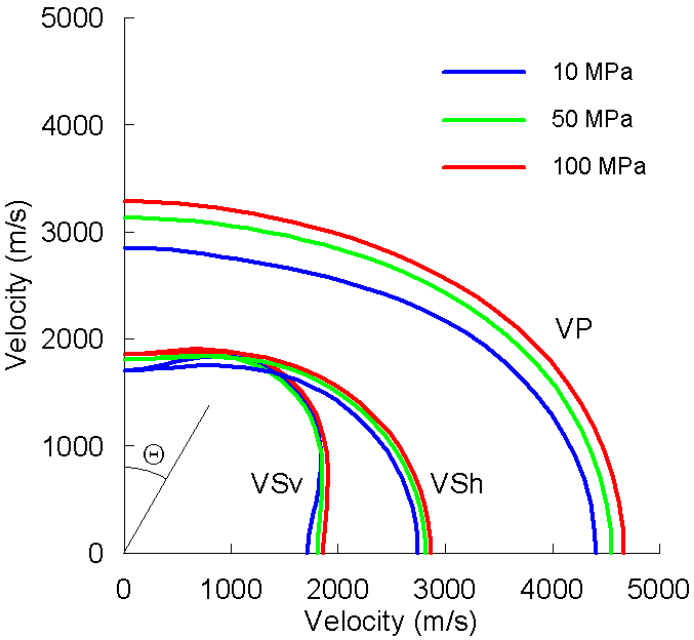

Figure 2 - Velocity map for waves propagating in a vertical plane of TH-26 shale sample.

Discussion of Results

The first point to be discussed is about the choice of an aspect ratio c/a = 1/10. Electronic microscopy images from these shale samples showed by Johnston & Christensen (1995) exhibit organic inclusions with this approximated aspect ratio. Figure 3, acquired for TH-26 shale sample under 50 MPa of hydrostatic pressure, shows that the proposed method is very sensitive to the parameter c/a, especially for a<10 (with c=1).

Table 3 -P, Sh and Sv wave anisotropies.

Sample	Pressure (MPa)	P Anis. (%)	Sh Anis. (%)	Sv Anis. (%)
TH-26	10	35.3	37.7	23.2
	50	31.1	35.8	17.3
	100	29.6	35.1	17.2
TH-51	10	34.0	35.5	23.3
	50	32.6	35.4	24.2
	100	30.9	34.9	24.0
NEW-2	10	25.1	22.8	13.8
	50	21.6	21.2	9.7
	100	20.1	20.0	8.3
NEW-3	10	27.1	22.8	11.0
	50	23.7	22.0	9.2
	100	21.9	21.0	9.0
NEW-5	10	26.0	20.0	5.9
	50	22.5	19.4	6.9
	100	20.7	18.5	5.8
NEW-7	10	24.2	20.2	6.2
	50	21.3	19.2	8.3
	100	19.8	18.5	8.2
ANT-1	10	26.6	25.5	9.1
	50	23.5	24.4	10.6
	100	21.8	23.9	11.9

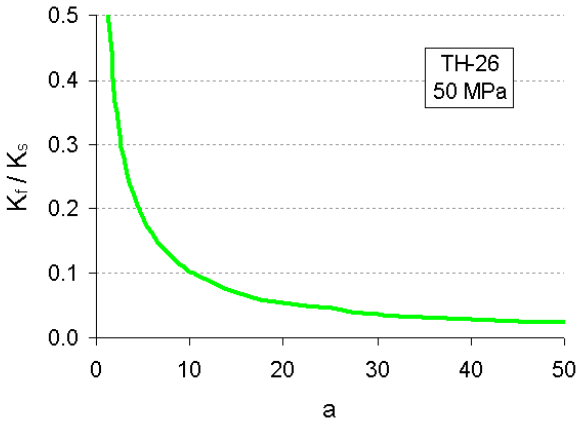

Figure 3 - Relationship between fluid/solid bulk modulus ratio and fluid inclusions diameter for TH-26 sample under 50 MPa.

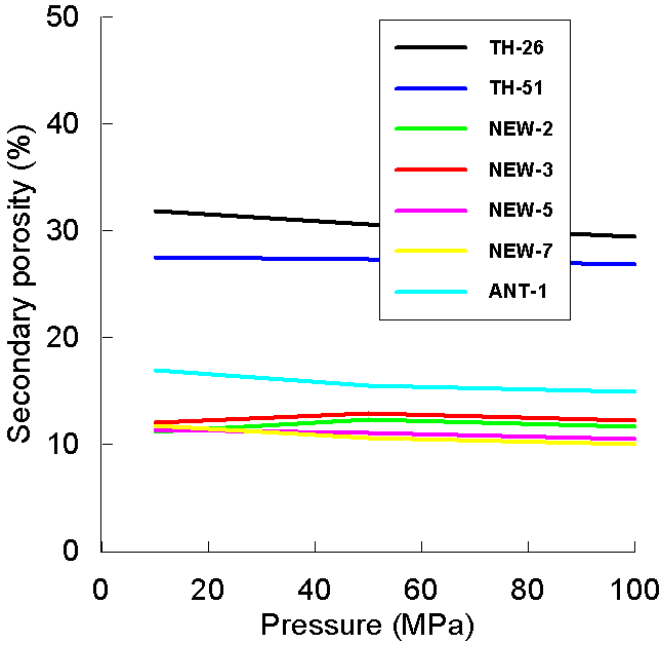

Figure 4 - Secondary porosity ϕ_c as a function of hydrostatic pressure.

But what about a ratio K_f/K_s approximately equal to 0.10? Depending on mineralogical composition of samples (see Table 1) and applying the model of Hill for an effective medium (Hill, 1952), a value for K_s around 40 GPa is reasonable if we consider that the rock solid frame is formed mainly of quartz and other hard minerals; whereas K_f may be near 5 GPa, if we consider that the organic matter inclusions are composed of a material like bituminous coal (Bourbié et al,1987). This yields a first approach to the ratio $K_f/K_s = 0.125$, what is no far from the initial suggested value $K_f/K_s = 0.10$. According to Table 2, samples TH-26, TH-51 and NEW-2 show values for K_f/K_s very close to this first approximation while the other samples show lower values for K_f/K_s. A possible explanation for these lower values of K_f/K_s may be due to saturation of organic inclusions by hydrocarbons, what can reduce the value of K_f. Another possible reason would be an increasing of K_s due to the presence of carbonate content in those samples, as can be seen in Table 1. Probably in those samples both mechanism actuate together to diminish the value of K_f/K_s.

Accepted the value for the aspect ratio c/a, one can proceed calculating, from $R_c = \phi_c/(c/a)$, the value for the secondary porosity ϕ_c, which in this method of analysis corresponds to the fraction of porous space occupied by the inclusions filled of organic matter.

Figure 4 shows values of secondary porosity ϕ_c, as function of hydrostatic pressure, calculated for the seven shale samples. There is an overall trend to diminish the values of ϕ_c with increasing of hydrostatic pressure. This may be interpreted as a mild effect of compression against inclusions of organic matter, resulting in a small reduction of their volume.

A more important observation is that the values of secondary porosity ϕ_c for samples TH-26 and TH-51 are higher than the values of ϕ_c for the other samples. There is such difference among the values of ϕ_c that allows an identification of two groups: one group of higher values of ϕ_c and other group of lower values of ϕ_c. The mineralogical and organic contents showed in Table 1 are depicted in Figure 5. In this figure, contents of silica, clay minerals, carbonate and organic matter are showed for each shale sample. From Figure 5 one may be observes a clear correspondence between the values of organic matter contents and the values of ϕ_c, as already expected.

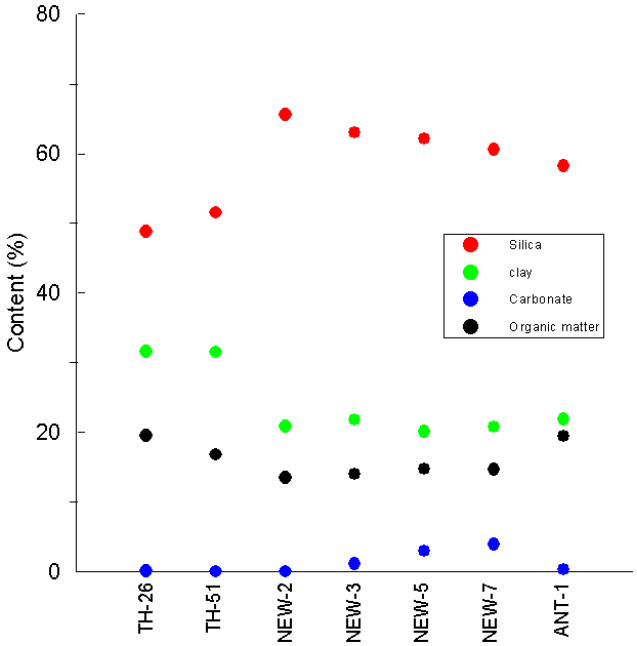

Figure 5 - Sample composition.

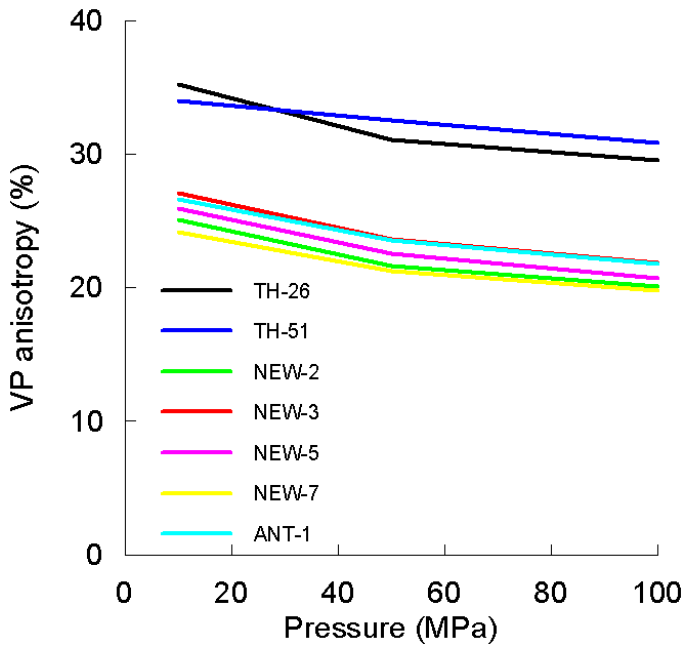

Figure 6 - Anisotropy variation of P wave velocity with pressure.

Figures 6, 7 and 8 show the behavior of P, Sh and Sv wave velocity anisotropies with the increasing of hydrostatic pressure over shale samples. These figures express the strong correlation between velocity anisotropy, especially in the case of P or Sh waves, and the secondary porosity showed in Figure 4. In other words, velocity anisotropy is strongly affected by content of organic matter and clay mineral. In the case of Sv wave this influence is minor and seems to be a higher dependency of Sv anisotropy on the function of the ratio K_f/K_s with pressure, showed in Figure 9.

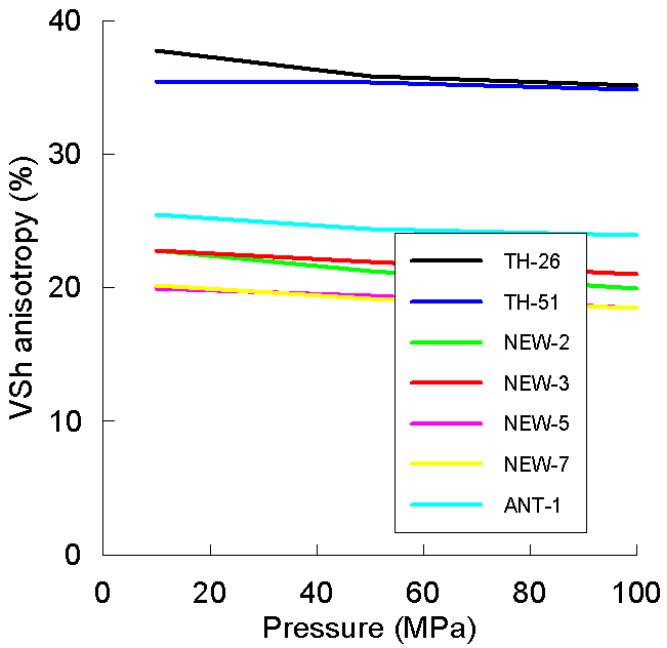

Figure 7 - Anisotropy variation of Sh wave velocity with pressure.

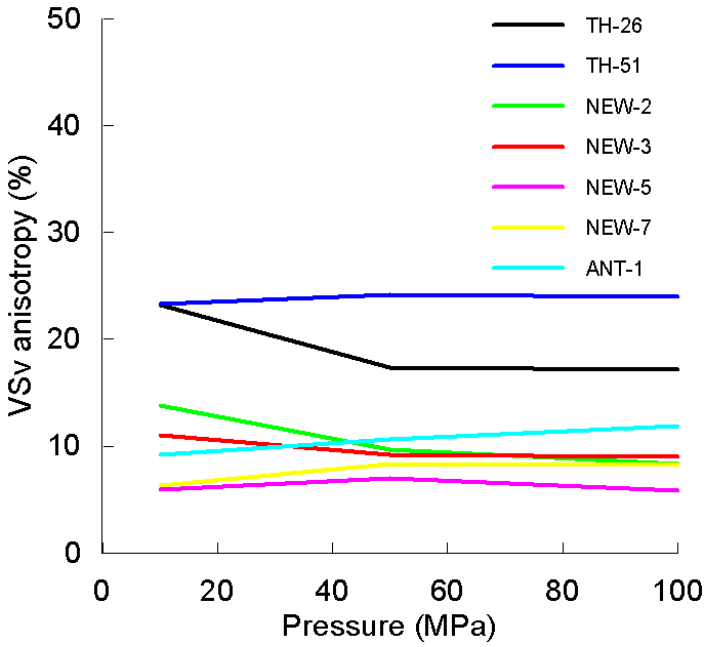

Figure 8 - Anisotropy variation of Sv wave velocity with pressure.

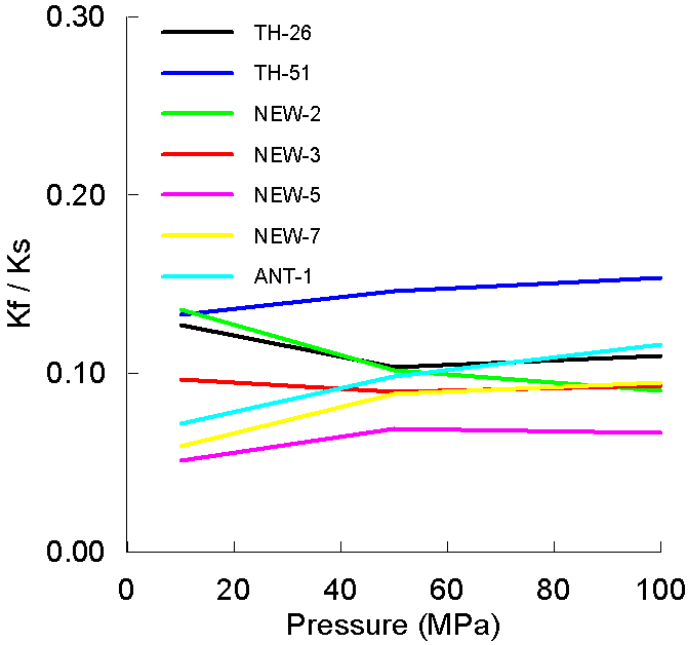

Figure 9 - K_f/K_s variation with pressure.

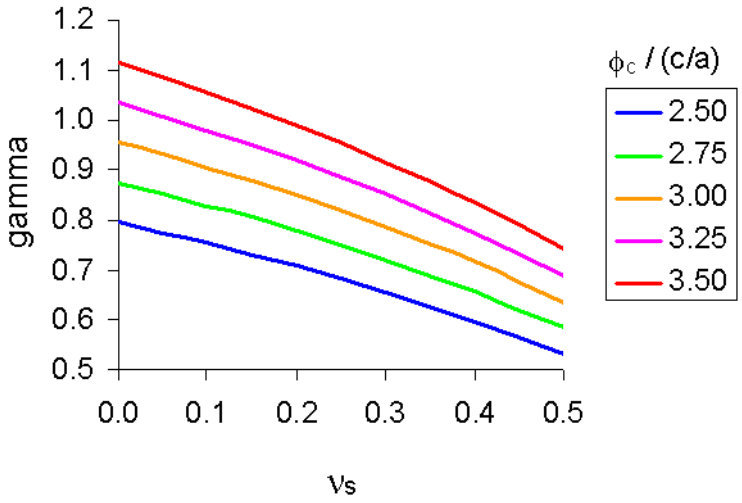

Figure 10 - Variation of γ anisotropy parameter with ν_s as a function of $\phi_c/(c/a)$.

Using Thomsen´s petrographical equations (eq. 4), an aspect ratio equal to 1/10 and adopting K_f/K_s = 5/40, the graphics of figures 10, 11 and 12 were built. In these figures one can see that, knowing the Thomsen´s anisotropy parameters ε, γ and δ, the values for the remaining petrophysical variables are restricted to a narrow possible range. That is, given a set of anisotropy parameters for a shale sample, probably there is only one other set of petrophysical variables (or some few sets very close among themselves) which honor those anisotropy parameters, according to Thomsen´s model.

Thence it follows that using the Thomsen´s model it is possible to evaluate shale petrophysical parameters if P and S velocities are known in three principal directions.

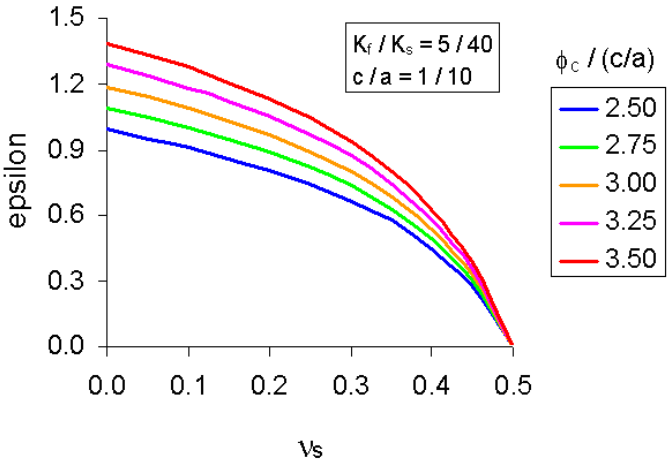

Figure 11 - Variation of ε anisotropy parameter with ν_s as a function of $\phi_c/(c/a)$.

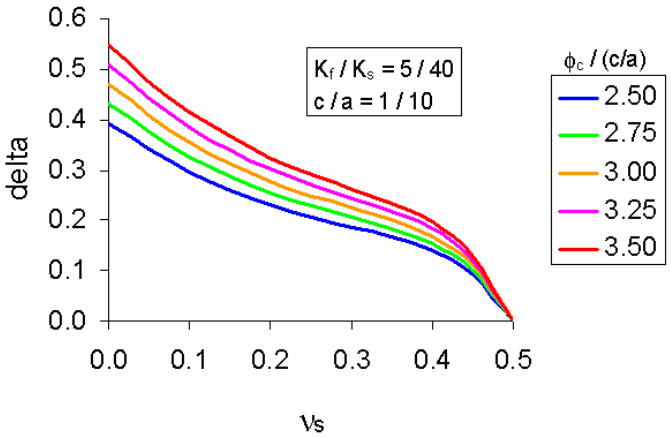

Figure 12 - Variation of d anisotropy parameter with ν_s as a function of $\phi_c/(c/a)$.

Conclusions

Although the Thomsen´s model has not be done to investigate composition and internal structure of shales, the results presented in this work suggest that it can be used with this finality.

The method of investigation here proposed is an interactive one. Initially, a value for aspect ratio of organic inclusions is assumed and, using this value, some petrophysical properties are calculated. Following, these petrophysical parameters are compared with those expected for the solid frame, organic inclusions and fluids contained in shale samples. This interactive process finishes when acceptable values are obtained for these properties.

This method may result in values which are an approximation of real values, since there are several sets of reasonable values which honor the data, even though all of them very close one to other. Due to this small possible range of properties, this method of investigation is not invalidated.

The variation of external hydraulic pressure over the shale samples resulted in a moderated effect on velocity anisotropy of the analyzed shale samples. The main factors which determine the level of velocity anisotropy are the chemical composition of the rock and its fluids besides the shape and distribution of organic matter filled inclusions inside the solid frame of rock.

Acknowledgments

This work was developed as part of the Project CTPETRO "Análise Petrofisica Integrada de Folhelhos", with financial support of PETROBRAS / FINEP and executed by the Department of Geology of Rio de Janeiro Federal University.

References

Bourbié, T., Coussy, O. and Zinszner, B., 1987, Acoustics of porous media. Éditions Technip. Paris.

Hornby, B. E., 1995, The elastic properties of shales - laboratory experiments: Quarto Congresso da SBGf, Resumos expandidos, Vol. 2, p793-796.

Hill, R., 1952, The elastic behavior of crystalline aggregate: Proc. Phys. Soc. London, A65, p349-354.

Johnston, J. E. and Christensen, N. I., 1995, Seismic anisotropy of shales: Journal of Geophysical Research, Vol. 100, Nº B4, p5991-6003, April.

Thomsen, L. A., 1986, Weak elastic anisotropy: Geophysics, Vol. 51, p1954-1966.

Thomsen, L. A., 1995, Elastic anisotropy due to aligned cracks in porous rock: Geophysical Prospecting, Vol. 43, p805-829.